

# Spasm of Near Reflex: Objective Assessment of the Near-Triad

Shrikant R. Bharadwaj,<sup>1,2</sup> Saujanwita Roy,<sup>1,2</sup> and PremNandhini Satgunam<sup>1,2</sup>

<sup>1</sup>Brien Holden Institute of Optometry and Vision Sciences, L V Prasad Eye Institute, Hyderabad, Telangana, India

<sup>2</sup>Prof. Brien Holden Eye Research Centre, Hyderabad Eye Research Foundation, L V Prasad Eye Institute, Hyderabad, Telangana, India

Correspondence: PremNandhini Satgunam, Brien Holden Institute of Optometry and Vision Sciences, L V Prasad Eye Institute, Road no. 2, Banjara Hills, Hyderabad, 500034 Telangana, India; [premnandhini@lvpei.org](mailto:premnandhini@lvpei.org).

**Received:** December 20, 2019

**Accepted:** May 21, 2020

**Published:** July 14, 2020

Citation: Bharadwaj SR, Roy S, Satgunam P. Spasm of near reflex: objective assessment of the near-triad. *Invest Ophthalmol Vis Sci.* 2020;61(8):18. <https://doi.org/10.1167/iovs.61.8.18>

**PURPOSE.** To characterize binocular steady-state accommodation, pupil and convergence responses (near triad) in spasm of near reflex (SNR) before and after optical and pharmacological intervention. To identify the putative source of SNR in the neural control schema of accommodation-vergence interaction using controls-engineering modeling.

**METHODS.** Near-triad of 15 patients with SNR (9 to 23 years) was recorded using an infrared photorefractor at 2m viewing distance for 120s during clinical presentation, after optical fogging intended to relieve spasm, *with* cycloplegia, post-cycloplegia and long-term follow-up visits. Data were also collected without cycloplegia in 15 age-matched controls. Schor (1999) model was used to computationally simulate accommodation and vergence responses of controls and SNR.

**RESULTS.** Both eyes of SNR exhibited significant myopia and refraction fluctuations (<1.0Hz) during clinical presentation [median (25<sup>th</sup> to 75<sup>th</sup> IQR) refraction: -1.7D (-3.2 to -0.8D); root mean squared (RMS) deviation: 1.1D (0.5 to 1.5D)], relative to controls [0.8D (-0.03 to 1.4D); 0.2D (0.1 to 0.3D)] ( $p < 0.001$ ). These decreased after optical fogging, largely eliminated *with* cycloplegia and partially re-appeared in the post-cycloplegia and follow-up visits. SNR responses could be modeled by increasing the gain and decay time of tonic accommodation, vis-à-vis, controls. Pupil and convergence responses in SNR were similar to controls at all visits ( $p > 0.1$ ).

**CONCLUSIONS.** Exaggerated fluctuations of steady-state accommodation may be a signature feature of SNR, even while their pupil and convergence responses may remain unaffected. These fluctuations may arise from the tonic accommodation controller, the properties of which could be potentially altered after optical fogging to relieve the disorder.

Keywords: accommodation, phasic, refractive fluctuations, spasm, tonic, convergence

When changing our viewing from a distant to a near object, the near-reflex response comprising of ocular accommodation, convergence and pupil miosis is elicited to achieve and maintain clear and single binocular vision.<sup>1</sup> The reverse—ocular disaccommodation, divergence, and pupil mydriasis—happens when viewing switches back to the distant target.<sup>1</sup> In a clinical condition called spasm of near reflex (SNR), these responses do not revert back to their relaxed state even if the person is looking at a distant object. Patients with SNR exhibit clinical signs of fluctuations in visual acuity, vacillating retinoscopy reflex, accommodative lead in dynamic retinoscopy, and symptoms of blurred vision and asthenopia.<sup>2-4</sup> Although several case reports have been reported about this condition (S. Roy et al., unpublished observations, 2019), its prevalence is rare<sup>5</sup> and etiology is unclear, with most studies postulating a psychogenic origin.<sup>2</sup> Cycloplegic eye drops, added plus lenses and vision therapy are some of the common management options for this condition (S. Roy et al., unpublished observations, 2019).<sup>2</sup> In a previous study done by us on 45 patients diagnosed with this condition (S. Roy et al., unpublished observations, 2019), we showed that 87% of patients with SNR could be

treated with a combination of cycloplegic refraction, a modified optical fogging technique<sup>6</sup> and vision therapy exercises (S. Roy et al., unpublished observations, 2019), either in the first post-cyclopentolate visit or with one-time use of atropine. In the remaining 13% of patients, atropine was required for prolonged use to relieve the spasm (S. Roy et al., unpublished observations, 2019).

In the present study, we quantitatively describe the characteristics of steady-state accommodation, convergence and pupil responses (the near-triad) in patients with SNR, vis-à-vis, age- and refractive error-matched control subjects. The objective assessment allows for clearer description and deeper understanding of the near-triad behavior during the active phase of the disorder, its changes with therapy and the long-term impact of therapy on the near-triad, beyond what can be obtained during routine clinical orthoptics evaluation. We also describe the results of a controls-engineering modeling exercise performed to explain the steady-state characteristics of accommodation and convergence obtained in these patients.<sup>7</sup> The model used here incorporates all aspects of our present understanding of blur-driven accommodation, disparity-driven convergence, and their

cross-coupled interaction (see Eadie and Carlin<sup>8</sup> for review). The modeling allows identification of putative elements in the neural control of accommodation and convergence that may explain the signs of the disorder and its changes with therapy. In the past, such models have formed the basis for understanding accommodation-convergence interactions in other non-strabismic binocular vision dysfunctions (e.g., convergence insufficiency).<sup>9</sup>

Apart from several case reports and case series on SNR that are reported in the literature,<sup>2-4</sup> only two previous studies quantified the characteristics of accommodation in patients with accommodative spasm.<sup>10,11</sup> The results showed that the mean accommodative state of these patients was more myopic and the steady-state fluctuations of accommodation in the 1–4 Hz frequency bandwidth were significantly higher in these patients compared with controls.<sup>10,11</sup> These studies, however, did not measure the pupil or convergence responses of their patients, and, hence, the synkinetic behavior of all three components of the near triad remains unknown in these patients. Furthermore, these studies did not attempt to computationally model the SNR responses or track its changes after intervention.

## METHODS

The study protocol adhered to the tenets of the Declaration of Helsinki, and it was approved by the Institutional Review Board of the L V Prasad Eye Institute, Hyderabad, India. The study commenced after all adults or the parents of all children younger than 18 years of age provided written informed consent. This study cohort comprised of last 15 of the 45 patients (median [25<sup>th</sup>–95<sup>th</sup> interquartile range] age, 13 years [9–15 years]) who were recruited for the aforementioned larger study from our group (S. Roy et al., unpublished observations, 2019). In that study, consecutive patients with a diagnosis or suspicion of SNR were enrolled. A comprehensive eye examination that included cycloplegic refraction (one drop of 1% cyclopentolate HCl eye drops and one drop of Tropicamide plus [0.8% Tropicamide and 5% phenylephrine HCl]) after assessing for the effect of cycloplegic action with a near acuity target. Diagnosis of SNR was confirmed primarily by the presence of hyperopic shift >2.00 D in cycloplegic retinoscopy when compared to the non-cycloplegic retinoscopy, with or without the disappearance of eso shift with cycloplegia. Additionally, signs of vacillating retinoscopy reflex, reduction/fluctuations in visual acuity that were not proportionate to the refractive error, were considered. No other systemic or ocular conditions were present in these patients. All the patients came for the postcycloplegic test (PCT), at two to three days after the first visit. If the spasm was present in the PCT visit, a modified optical fogging technique was attempted to relieve the spasm.<sup>6</sup> In this technique a plus power (+2.50DS) about the value of negative relative accommodation, was given to the patient in a trial frame and the patient was made to read a book for about 30 minutes.<sup>6</sup> After this, binocular defogging was done while simultaneously encouraging the patient to read from the top-most line of the visual acuity chart. If the accommodation relaxes, the patient will be able to read to about 20/20 (i.e., 0 logMAR), with a refractive error value that would be closer to the cycloplegic refraction.<sup>6</sup> Those patients whose accommodation was relaxed in the first PCT visit were categorized to have mild SNR (S. Roy et al., unpublished observations, 2019). For those patients without relief, atropine refraction was done. Eye drops of 1% atropine sulfate were prescribed twice a

day for three days, and the patient was called for atropine refraction to be performed on the fourth day. In the post-atropine visit (two weeks after the atropine refraction) if their spasm was relieved with or without the modified optical fogging technique, they were categorized to have moderate SNR (S. Roy et al., unpublished observations, 2019). If they continue to have the spasm despite these interventions, they were deemed to have severe SNR (S. Roy et al., unpublished observations, 2019). Such patients were advised to use atropine/homatropine eye drops (1% atropine sulfate once a week or 2% homatropine hydrobromide twice a day) for a month and asked to come for a follow-up.

Because this study aimed at reporting the characteristics of the near triad during the manifest phase of the disorder, the recruitment of patients into the study could be made only on the suspicion of SNR and not on the basis of a confirmed diagnosis. All patients recruited for this study eventually had a confirmed diagnosis of this dysfunction. The demographic details, along with refractive error and visual acuity of the 15 patients enrolled for this study, are shown in Table 1. None of the patients in this cohort had a previously confirmed diagnosis of SNR or have had a cycloplegic examination before study recruitment. Standard clinical management was followed in all patients, with no influence of the study protocol/results on their care. Fifteen age-matched control subjects (15 years [10–19 years]) with emmetropic manifest refraction, uncorrected distance acuity of 20/20 (i.e., 0 logMAR) or better in each eye and with normal binocular vision were also recruited for the study from among the staff and students of the institute and from patients who attended the clinic for a routine eye examination. All the clinical examinations were performed by one of the two senior optometrists with more than three years of experience working in the Binocular Vision and Orthoptics clinic.

## Measurement of the Near-Triad

Data were collected on each patient on the following five occasions: (1) at the time of their presentation to clinic with SNR (denoted as precycloplegia), (2) after the optical fogging technique that was intended to relieve their spasm (denoted as postoptical fogging), (3) with pharmacological cycloplegia (denoted as with cycloplegia), (4) during the PCT visit to clinic after wearing-off of cycloplegia (denoted as PCT), and (5) during the long-term follow-up visit of the patient, a few weeks to months after their initial visit (denoted as follow-up). These data were compared against the noncycloplegic data of age- and refractive error-matched control subjects with no signs and symptoms of SNR. On all these occasions, the patients and control subjects steadily fixated on a thin vertical line target at 2 m viewing distance binocularly without their refractive error correction in an otherwise dimly lit room (~15–20 cd/m<sup>2</sup>). The target had broadband spatial frequency content and subtended 2.8° height × 0.5° width at the nodal point of the eye from this viewing distance. Their steady-state accommodation, pupil diameter, and convergence were recorded continuously for 120 seconds and in-sync with each other using the PowerRef 3 eccentric, infrared photorefractor (Plusoptix GmbH, Nuremberg, Germany) at 50 frames per second sampling rate. All data were collected using the standard settings of the photorefractor as recommended by the device manufacturer. Detailed evaluation of the PowerRef 3 as a tool to measure the near-triad responses is already available in the literature.<sup>12-14</sup> The photorefractor measures the refractive power of the eye by converting the luminance slope

TABLE 1. Demographic and Clinical Details of Patients With SNR Who Participated in This Study

Patient Number	Age   Gender	Clinical Severity of SNR	SER   VA Pre-cyclo	SER   VA Post-fogging	SER   VA With Cycloplegia	SER   VA PCT	SER   VA Follow-up
S1	14   F	Mild	-7.9   0.3	0.5   0.1	0.5   NR	+1.00   0.0	0.0   0.0
S2	19   M	Mild	-1.8   1.6	0.5   0.0	0.6   0.0	-1.5   0.3	-2.5   0.9
S3	15   M	Mild	-5.5   1.1	0.5   0.02	0.3   0.1	0.0   0.0	0.5   0.0
S4	22   M	Mild	-3.0   0.0	0.8   0.0	0.5   0.0	0.5   0.1	0.0   0.0
S5	14   F	Moderate	-5.0   0.7	0.5   0.6	1.9   0.1	-1.8   0.4	-1.8   0.0
S6	15   M	Mild	-1.3   0.2	0.5   -0.1	1.0   NR	0.5   0.0	No visit by patient
S7	11   M	Mild	-3.0   0.1	0.5   0.04	0.0   0.0	-4.5   0.3	0.8   0.0
S8	10   F	Mild	-5.0   1.0	0.5   0.1	1.25   NR	0.75   0.02	0.0   0.0
S9	9   M	Mild	-8.5   1.1	0.5   0.5	0.0   0.4	1.0   0.3	0.8   0.1
S10	13   F	Mild	-4.0   0.4	0.5   0.0	0.0   0.1	-3.0   0.3	No visit by patient
S11	12   M	Mild	-2.0   0.9	0.8   0.0	0.25   NR	0.75   0.0	0.75   0.0
S12	13   F	Mild	-6.0   0.4	0.5   0.1	1.5   NR	0.0   0.3	0.8   0.0
S13	12   M	Moderate	-4.0   1.4	NR	0.0   NR	-4.0   1.0	0.0   0.0
S14	12   M	Moderate	-5.5   0.8	NR	1.0   0.0	-6.0   0.9	0.5   0.0
S15	23   M	Moderate	-3.0   0.4	0.5   0.0	2.0   0.0	0.5   0.2	-1.0   0.3
Median (IQR)	13 (12–15)		-4.0 (-3.0 to -5.5)   0.7 (0.3 to 1.1)	0.5 (0.5 to 0.8)   0.2 (0 to 0.1)	0.5 (0.2 to 1.1)   0.1 (0 to 0.1)	-1.5 (-3.5 to 0.3)   0.3 (0.3 to 0.5)	0.0 (0 to 0.8)   0 (0 to 0)

Only data from the left eye are shown here. The patient's age, high-contrast distance VA and SER are represented in years, logMAR units, and diopters, respectively. The visual acuity represents the presenting visual acuity in the pre-cyclo visit and the best-corrected visual acuity in all subsequent visits. All visual acuity and refraction values were obtained during the clinical examination. Visual acuity was obtained using an electronic logMAR acuity projection chart (Complog, Ver. 1.3.25.0, Bristol, UK) with three of five optotypes correctly identified as the standard endpoint of acuity testing.<sup>23</sup> Refraction values were obtained either from a closed-field autorefractor (Unique-RK, URK-800F, Korea; average of three measurements) or from the approximate correction that gave a reversal in the retinoscopy reflex. VA, visual acuity; SER, spherical equivalent of refractive error; NR, no data recorded in that instance.

of the reflected infrared (IR) light formed across the pupil into diopters using an in-built defocus calibration factor.<sup>15–17</sup> It is recommended that each subject's raw data be scaled using their own custom-derived calibration factor or an average ethnicity-specific calibration factor to obtain accurate measures of changes in refractive power.<sup>18</sup> Because individual calibration was not possible here because of the subject's unsteady manifest refraction, the raw data were scaled using the average calibration factor for subjects of Indian ethnicity from an earlier study by Sravani et al.<sup>18</sup> The individual eye's gaze position is recorded by the photorefractor by tracking the relative separation between the first Purkinje image and the entrance pupil center and applying an in-built Hirschberg ratio (11.8°/mm) to convert this separation into angular units of degrees.<sup>19</sup> Binocular convergence is then derived by taking the difference between the two eyes' gaze positions at each frame. The inbuilt value of Hirschberg ratio used by the photorefractor does not show any significant biases and therefore no further scaling of the raw gaze position or convergence data were performed.<sup>19</sup> Pupil diameter is calculated by the photorefractor for each eye, again in-sync with accommodation and gaze position, by detecting the pupil edges using inbuilt image processing algorithms.

### Control Experiment

Patients with SNR typically show a manifest myopic refraction that changes to reduced myopia, emmetropia or hyperopia with cycloplegia.<sup>2,4</sup> The control subjects that participated in the main experiment were all emmetropes, and it was therefore not clear whether the differences in data observed between patients and controls, especially the refractive fluctuations, were due to differences in the underlying manifest refraction or whether it was something unique to the pathophysiology of SNR. To address this

issue, a control experiment was performed by measuring the pattern of steady-state accommodation, pupil and convergence in five myopes (9–15 years; manifest refraction: -1.0 to -4.0D) and five hypermetropes (11–14 years; +0.5 to +2.5 D) who did not exhibit any signs and symptoms of SNR. All details of data collection and analyses were similar to the main experiment.

### Data Analyses

Data analysis was performed using Matlab (R2016a; The MathWorks Inc, Natick, MA, USA). The raw data were smoothed using a 100-ms-long running-average filter and then divided into three 20.4-second-long (i.e., 1024 points) epochs for analysis. The characteristics of steady-state accommodation, convergence, and pupils in each epoch were described in the time domain using the mean and root mean squared (RMS) deviation of the data and in the temporal frequency domain as the fast Fourier transform (FFT)-derived amplitude spectrum of the data. The results of the control experiment are described only in the time domain. Kolmogorov-Smirnov testing indicated that most outcome variables in this study did not follow a normal distribution. The nonparametric Friedman test and the post-hoc Dunn test compared data within and across groups. Statistical significance was set at  $P < 0.05$ .

### Controls Engineering Modeling of Accommodation and Convergence

A well-established controls-engineering model of accommodation-convergence interaction described by Schor was used for modeling the behavioral responses of controls and patients with SNR (Fig. 1).<sup>7</sup> Briefly, the model describes accommodation and convergence to step





**TABLE 2.** Parameters Used in the Controls Engineering Model to Simulate the Steady-State Responses of Accommodation and Convergence in Controls and Patients With SNR

Parameters	Accommodation	Convergence
Simulation of a control subject		
Stimulus	0.5 D	0.5 MA
Dead-space operator	-0.25D to +0.25D	-0.01 MA to +0.01MA
Response latency	300 ms	200 ms
Phasic controller gain   time constant	2.5 (unitless)   5sec	2.5 (unitless)   5sec
Tonic controller gain   time constant	1.5 (unitless)   20sec	1.5 (unitless)   20sec
Plant gain   time constant	0.25 (unitless)   0.17sec	0.3 (unitless)   0.14sec
Feedback gain	1.0 (unitless)	1.0 (unitless)
AC/A ratio	0.7 MA/D	—
CA/C ratio	—	0.9 D/MA
Bias (Spectacle or Phoria)	0D	0MA
Saturation element range	-15D to +15D	-2.5 MA to +5 MA
Response amplitude	0.44D	0.46 MA
RMS deviation	0.07D	0.08 MA
Oscillation frequency	0Hz	0 Hz
Simulation of a subject with SNR		
Tonic controller gain   time constant	150 (unitless)   200 sec	1.5 (unitless)   20 sec
Response amplitude	0.56 D	0.36 MA
RMS deviation	0.93 D	0.38 MA
Oscillation frequency	0.35 Hz	0.20 Hz
Simulation of a subject with partially corrected SNR		
Tonic controller gain   time constant	30 (unitless)   40 sec	1.5 (unitless)   20 sec
Response amplitude	0.62D	0.40 MA
RMS deviation	0.37D	0.08 MA
Oscillation frequency	0.35 Hz (with amplitude dampening over time)	0 Hz

The parameters used in the control subject were obtained from Schor et al.<sup>7</sup> with slight modifications to qualitatively match the empirical responses. The model parameters were then adjusted until the simulations qualitatively resembled the accommodation-convergence responses of patients with SNR. The response output of each model simulation is also shown in this table.

mild SNR, and the remaining four had moderate SNR, based on the criteria described earlier (S. Roy et al., unpublished observations, 2019; Table 1). All patients were relieved of SNR after cycloplegia or with the modified optical fogging.

### Raw Data of Manifest Refraction, Pupil Diameter and Convergence Eye Position

Relative to a control subject (Fig. 2A), the raw data of a representative patient with SNR showed large fluctuations in manifest refraction at the time of presentation, and it was reduced significantly after the modified optical fogging and with cycloplegia (Fig. 2, top row). The steady-state pupil diameter of the patient on the first two occasions showed the characteristic hippus, similar to the control subject (Fig. 2, middle row). As expected, the patient's pupils dilated, and the hippus was abolished with cycloplegia (Fig. 2D). The manifest refraction and pupil diameter of the patient were very similar in both eyes, much like in controls (Fig. 2, top and middle rows). The monocular eye position and convergence of the patient and the control subject were similar in all sessions, sans any fluctuations (Fig. 2, bottom row). The data from the PCT and follow-up visit of this patient resembled the control data and, hence, are not shown separately.

### Individual Trends in the Steady-State Characteristics of the Near Triad

Each data point in Figure 3A indicates the trend in steady-state manifest refraction and their RMS deviation (Fig. 3B) at the time of clinic presentation, after optical fogging, with cycloplegia, PCT and the follow-up visit, in that order. Gener-

ally, in all patients (except S2 and S5), the manifest refraction was most myopic, and the RMS deviation of refraction was largest at the time of clinic presentation (Fig. 3).

The manifest refraction shifted to its most hyperopic value and the RMS deviation was least with cycloplegia (Fig. 3). The optical fogging technique elicited variable responses across patients, with the general trend of the manifest refraction shifting in the hyperopic direction and the RMS deviation reducing following this technique (Fig. 3). These changes, however, did not quite reach the level of cycloplegia in any patient (Fig. 3). In two patients (S2 and S5), the manifest refraction became more myopic, and the RMS deviations increased after optical fogging (Fig. 3). In all patients (data not available for S1, S10 and S13), the manifest refraction shifted back in the myopic direction and the RMS deviation increased during the PCT visit, suggesting a rebound of spasm in these patients after relief from cycloplegia (Fig. 3). Follow-up data were available on 11 patients (data not available for S6, S7, S10, and S15), and there was a trend for the manifest refraction to be less myopic and the RMS deviation to be smaller than the time of first presentation or during the PCT visit (Fig. 3). Overall, the trends from the left and right eye of all patients were very similar to each other. Pupil diameter and convergence did not show any significant trend across the different sessions.

### Median Trends in the Steady-State Characteristics of the Near Triad

Because data from the two eyes of patients with SNR were similar to each other, only results from the left eye are reported here (Fig. 4). The manifest refraction and its RMS

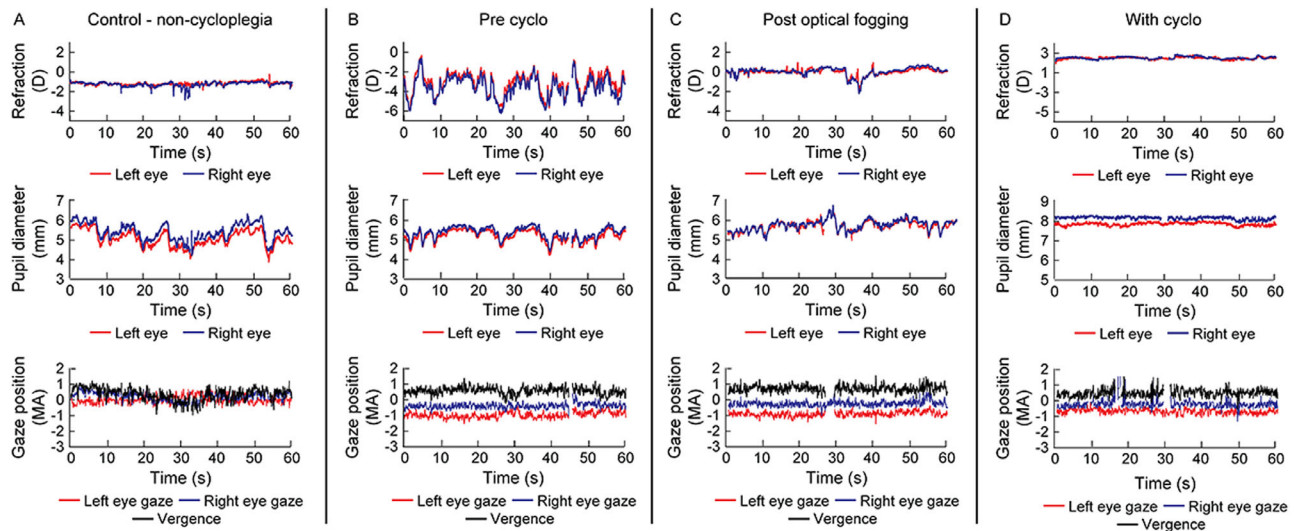


**FIGURE 2.** Raw traces of right and left eye manifest refraction, pupil diameter and monocular gaze positions and binocular convergence plotted as a function of time for one representative control subject without cycloplegia (**A**) and one representative patient with SNR (**B–D**). Data for the first 60 seconds of the total 120 seconds of recording is shown here. The data trends were similar for the first and second epochs of recording. Negative values of manifest refraction and gaze position indicate myopia and convergence, respectively. Missing data chunks are due to blinks or values that were outside the instrument's linear operating range. The ordinate axes for manifest refraction and pupil diameter have different ranges across panels to clearly show the raw data.

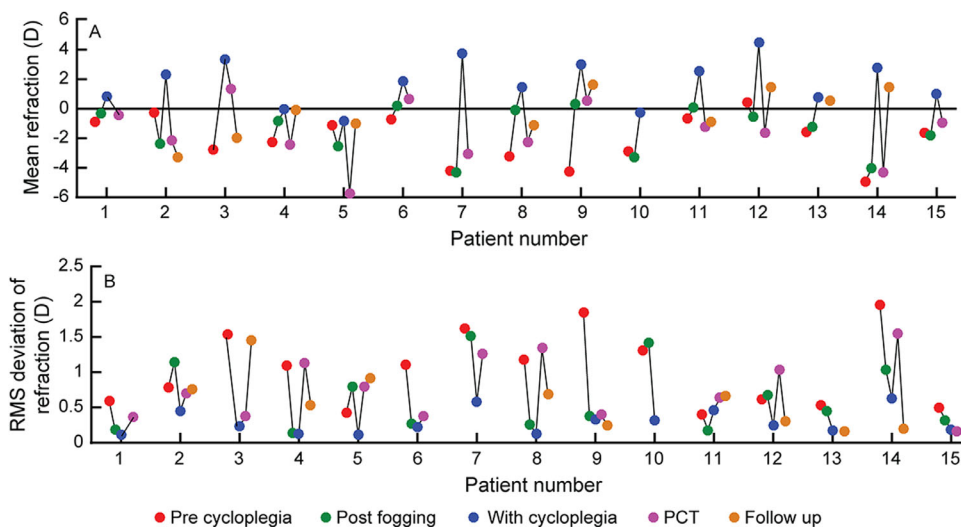


**FIGURE 3.** Mean manifest refraction (**A**) and the RMS deviation of manifest refraction (**B**) of the left eye of individual patients measured using the Plusoptix PowerRef 3 photorefractor. Each color-coded data point is indicative of the different conditions that the patient participated in. The *solid horizontal line* in panel **A** indicates emmetropic manifest refraction. The data from the right eye were very similar to the left eye and, hence, are not shown in this figure.

deviation collected were overall statistically significantly different across different sessions ( $df = 89$ ;  $\chi^2 \geq 42.4$ ;  $P < 0.001$ , for both) (Fig. 4). For both parameters, the control data were statistically significantly different from all sessions ( $Q \geq 3.4$ ;  $P < 0.001$ ), except the PCT and the long-term follow-up sessions ( $Q \leq 1.9$ ;  $P > 0.05$ ). The data at the time of clinic presentation and after optical fogging were significantly different only from the cycloplegia data ( $Q \geq 4.4$ ;  $P < 0.001$ ) but not from each other ( $Q \leq 2.3$ ;  $P > 0.05$ ). The PCT and the long-term follow-up visit sessions were not significantly different from each other ( $Q \leq 2.9$ ;  $P > 0.05$ ).

The median pupil diameter and its steady-state fluctuation were overall statistically significantly different across the different sessions in patients with SNR ( $df = 89$ ;  $\chi^2 \geq 22.3$ ;  $P < 0.001$ , for both). Pupil responses after cycloplegia was statistically significantly different from all other sessions ( $Q \geq 3.3$ ;  $P < 0.001$ ), whereas all other comparisons were not significantly different from each other ( $Q \leq 1.5$ ;  $P > 0.05$ ). Convergence showed no statistical significance in the data across the different sessions in patients with SNR ( $df = 89$ ;  $\chi^2 = 4.1$ ;  $P = 0.54$ ).

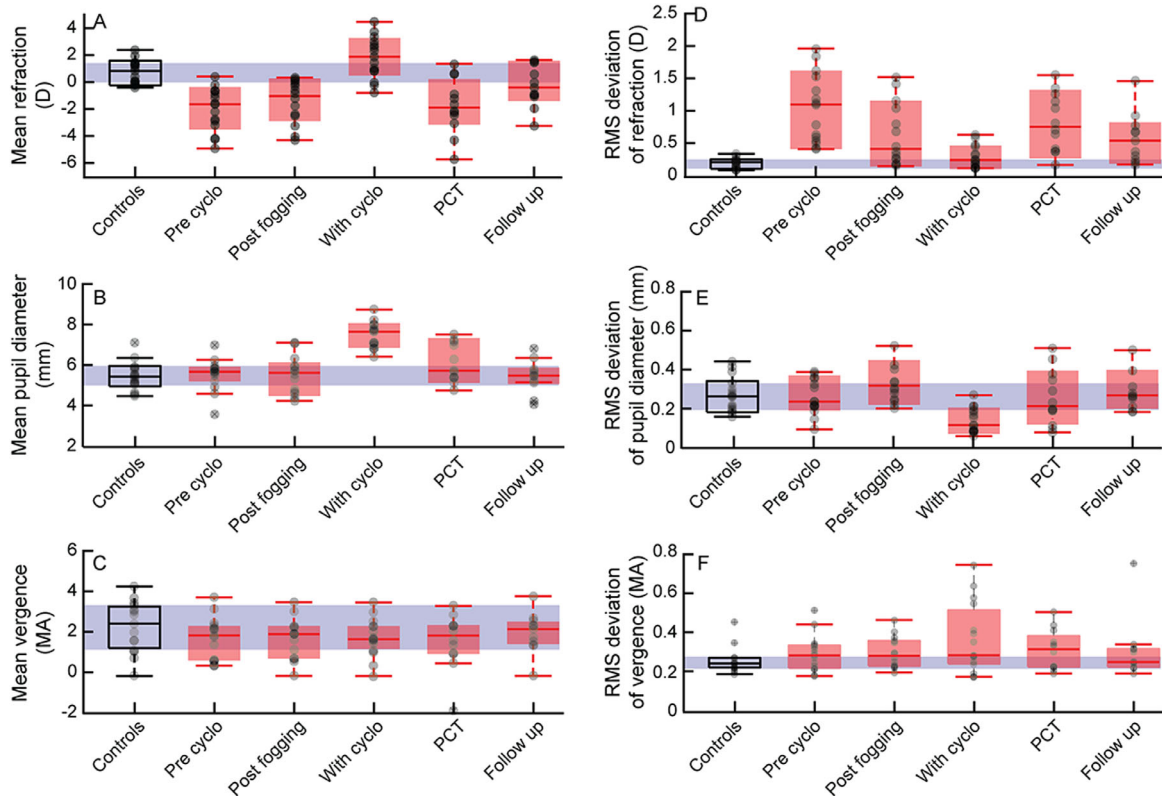


**FIGURE 4.** Box and whisker plots of the left eye's steady-state manifest refraction and RMS deviation, pupil diameter and convergence for controls and for the different sessions in patients with SNR. The *solid horizontal line* within the box indicates the group median, lower and upper edges of the box indicate the twenty-fifth and seventy-fifth interquartile range (IQR), and lower and upper whiskers show the first and ninety-ninth quartiles. The *filled circles* represent individual data points. The *gray band* across each panel represents the IQR of controls.

### Temporal Characteristics of the Steady-State Responses of Near Triad

The amplitude spectrum of the steady-state responses shown in Figure 2 for the control subject and patient with SNR is presented in Figure 5. As reported previously,<sup>24</sup> the amplitude spectrum of manifest refraction for the control subject showed the characteristic low temporal frequency microfluctuations, with most of the energy distributed at frequencies  $<0.5$  Hz (Fig. 5A). The data of the patient with SNR at the time of presentation showed exaggerated amplitudes of fluctuations, with most of the energy distributed at frequencies  $<1$  Hz (Fig. 5A). The magnitude of these fluctuations reduced to the level of the control subjects after the modified optical fogging technique, and they were largely eliminated with cycloplegia (Fig. 5A). The results of the group data of the temporal frequency analysis was very similar to that obtained for RMS deviations (Fig. 5D). Statistical analyses are therefore not presented separately here.

The amplitude spectrum of pupil fluctuations showed increased energy at temporal frequencies  $<0.5$  Hz, as reported previously,<sup>25</sup> and this trend was not qualitatively different between controls and patients with SNR at the time of their clinic presentation or after optical fogging (Figs. 5B and 5E). Much like the manifest refraction, the amplitude of the temporal fluctuations in pupil diameter was largely eliminated with cycloplegia (Figs. 5B and 5E) ( $Q \geq 3.2$ ;  $P < 0.001$ ). The amplitude spectrum of convergence for controls

and patients also showed an increase in energy levels at the low temporal frequencies (Figs. 5C and 5F), but this was not as prominent as what was seen for manifest refraction or pupil diameter. The change in the amplitude spectrum of patients across different sessions was also not as prominent as the other two components of the near triad (Figs. 5C and 5F).

### Relation Between the Mean Data and RMS Fluctuations of the Near Triad

Across the data of controls and patients combined, the magnitude of RMS deviation of manifest refraction increased with the mean magnitude of manifest refraction (Spearman's correlation coefficient;  $r = -0.74$ ;  $P < 0.001$ ) (Fig. 6A). Patients with greater magnitude of manifest myopia tended to show larger fluctuations in their refraction, relative to those with smaller magnitudes of manifest myopia. A reduction in the magnitude of manifest myopia with optical fogging or with cycloplegia was also associated with a corresponding reduction in magnitude of the refraction fluctuations. Pupils also showed a significant negative correlation between the mean and the RMS deviation ( $r = -0.40$ ,  $P < 0.001$ ) (Fig. 6B), but this relation was largely driven by the increased pupil diameter and reduced RMS deviations with cycloplegia (Figs. 6B and 6E). No such relation existed for convergence ( $r = -0.21$ ;  $P = 0.10$ ) (Fig. 6C).

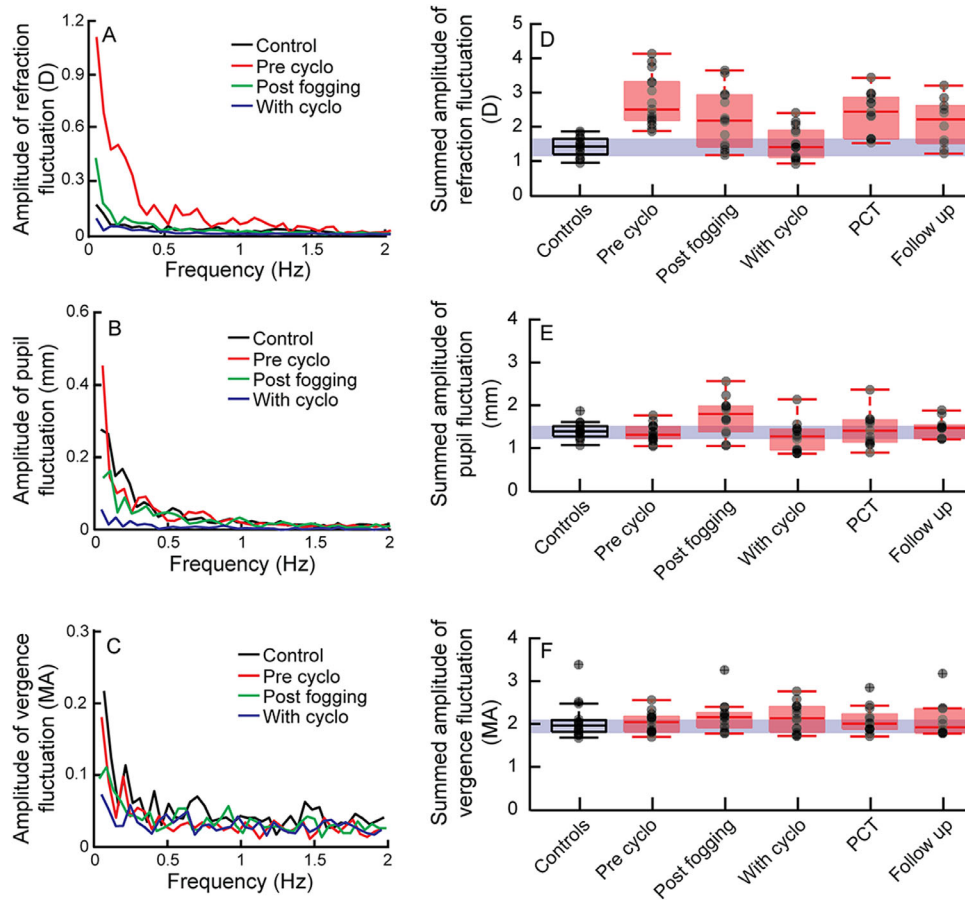


**FIGURE 5.** Amplitude spectrum of steady-state manifest refraction, pupil diameter and convergence for one representative case with SNR and one control subject. Right panels show box and whisker plots of summed amplitude of fluctuations for manifest refraction, pupil diameter, and convergence.

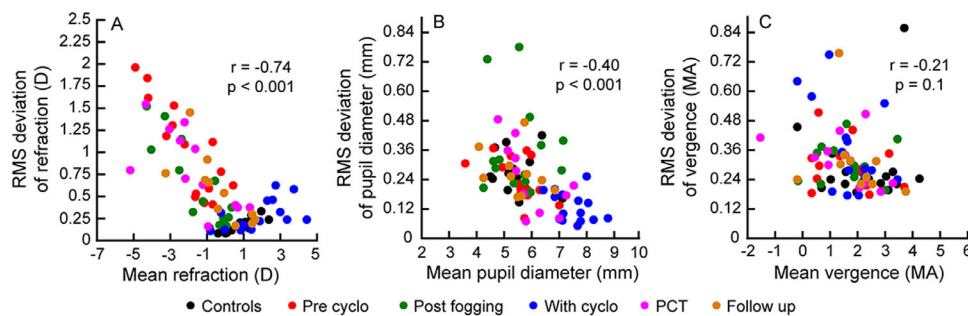


**FIGURE 6.** Scatter diagram of manifest refraction (A), pupil diameter (B), and convergence (C) plotted against their corresponding RMS deviations for controls and for the different sessions in patients with SNR.

### Control Experiment

The manifest refraction of myopic controls was in the same range as the patients with SNR, whereas the manifest refraction of hyperopic and emmetropic controls were significantly different from patients and the myopic controls (Fig. 7A). The RMS deviation of the all three control groups (emmetropic, myopic and hyperopic) were, however, significantly smaller than those of patients ( $P < 0.001$ ) (Fig. 7A). There was no difference in the mean and RMS deviation of pupil diameter ( $P = 0.43$ ) (Fig. 7B) and convergence ( $P$

$= 0.55$ ) (Fig. 7C) of controls and patients. The pupil and convergence components of the near-triad do not appear to show any sign of dysfunction in this cohort of patients.

### Controls Engineering Model Simulations of Accommodation and Convergence

The model simulations produced a stable steady-state accommodative and convergence response for controls using the parameters shown in Table 2 (Fig. 8A). The



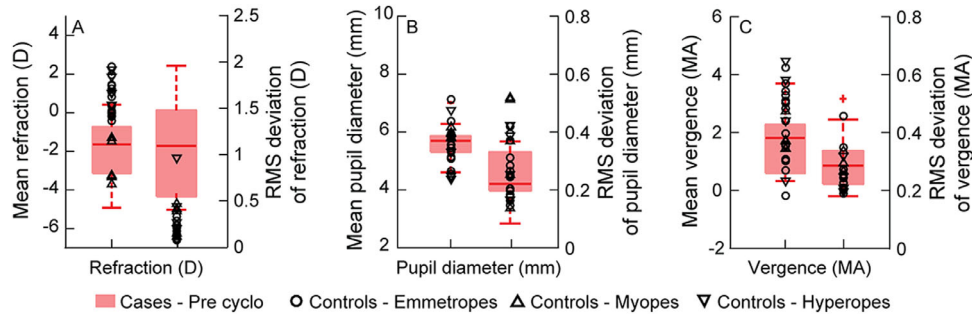


**FIGURE 7.** Comparison of steady-state and RMS deviations of accommodation, pupil diameter, and convergence in emmetropic, myopic, and hyperopic controls versus patients with SNR at the time of clinical presentation. The individual data points show responses from the three control groups whereas the box and whisker plots show data of patients with SNR. The box and whisker plot is the same data as shown in Figure 4. In all the panels, the ordinate axis on the left, the left box and whisker plot and the individual data points of the controls corresponds to the mean data, whereas the ordinate axis of the right along with the right box and whisker plot and individual data points of the controls corresponds to the RMS deviations.

output of the phasic accommodation controller was prominent during the early phase of step response, and this was replaced by the sustained output of the tonic accommodation controller (Fig. 8B). The exaggerated fluctuations in the steady-state refraction of patients with SNR were successfully simulated by increasing the gain and lengthening the decay time constant of the tonic accommodation controller (Table 2). The simulations qualitatively matched the behavioral responses of patients for a 100-fold increase in gain of tonic accommodation and tenfold lengthening of its decay time constant (Table 2, Fig. 8C). Convergence position also showed fluctuations in the steady-state response, but they were relatively minor compared with accommodation (Fig. 8C). The fluctuations in accommodation largely arose from the instability of the tonic accommodation controller's output (Fig. 8D). A reduction in the gain and a shortening of the decay time constant of this controller expectedly reduced the amplitude of the accommodation fluctuations. Example of responses with an 80-fold reduction in the properties of the tonic accommodation controller is shown in Table 2 and Fig. 8E. The minor fluctuations in the convergence were also eliminated in this process (Fig. 8E). Changes to other components of the model did not generate responses that resembled the behavioral data of patients with SNR.

## DISCUSSION

### Refraction Fluctuations in SNR

Most of the interesting findings in the near-triad of patients with SNR who were recruited for this study appear to revolve around the manifest refraction component. Of these, the exaggerated fluctuations in manifest refraction appear to be a pathognomonic sign of spasm in this disorder (Fig. 2). Such fluctuations have been observed clinically as a vacillating reflex in retinoscopy that makes the determination of the endpoint of objective and subjective refraction quite challenging and elusive.<sup>2,4</sup> Because these fluctuations occur with a definite temporal periodicity, as determined in this study (Figs. 2 and 5), an attempt to neutralize the retinoscopy reflex is often futile and meaningless. Patients subjectively report a temporal fluctuation in their vision as a part of their presenting history and clinicians also often report the visual acuity of these patients to vary by several lines during examination. This variability in response may reflect an underlying

fluctuation in retinal image quality owing to the fluctuation in refraction. Visual acuity tends to deteriorate in the presence of purposely induced temporal variations in optical blur in otherwise normal individuals,<sup>26</sup> and a similar response is expected in patients with SNR because of their innate refraction fluctuations. The loss of visual acuity of the patients enrolled in this study at the time of clinical presentation could therefore be due to a combination of the manifest myopic refraction and its temporal fluctuations (Table 1, Figs. 2–5). The improvement in acuity to  $\sim 0$  logMAR ( $\sim 20/20$ ) after optical fogging and with cycloplegia may be due to both the overall refraction values tending towards emmetropia and a reduction in the fluctuations, as noted in the present study (Table 1, Figs. 2–5). The exact relation between the mean refraction values, its fluctuations and visual acuity measurements in SNR are currently being systematically explored in our laboratory.

Such fluctuations in refraction during retinoscopy or a variable patient response during acuity testing may be used to suspect SNR, and appropriate workup may be pursued for diagnosis confirmation. These clinical observations could be combined with objective measures of the near triad using photorefractometry to facilitate the diagnosis of SNR and monitor its changes with therapy. The temporal fluctuations in manifest refraction captured using photorefractometry could be a potential marker for screening pseudomyopia and differentiating it from true myopia. Toward this end, the control experiment performed here does show that unlike patients with SNR, age-matched myopes of similar magnitude do not show any fluctuations in their manifest refractive error (Fig. 7A).

### Putative Source of Refraction Fluctuations in SNR

The near-elimination of these refraction fluctuations after cycloplegia suggest that they largely arise from periodic contraction and relaxation of the ciliary muscle. The refraction fluctuations in SNR have the same temporal frequency range ( $< 1$  Hz) as the low-frequency component of physiological accommodative microfluctuations (Fig. 5).

It is therefore possible that these refraction fluctuations are related mechanistically to the physiological accommodative microfluctuations but are just exaggerated in magnitude in SNR. Further experiments are required to establish the mechanistic similarity between the two fluctua-

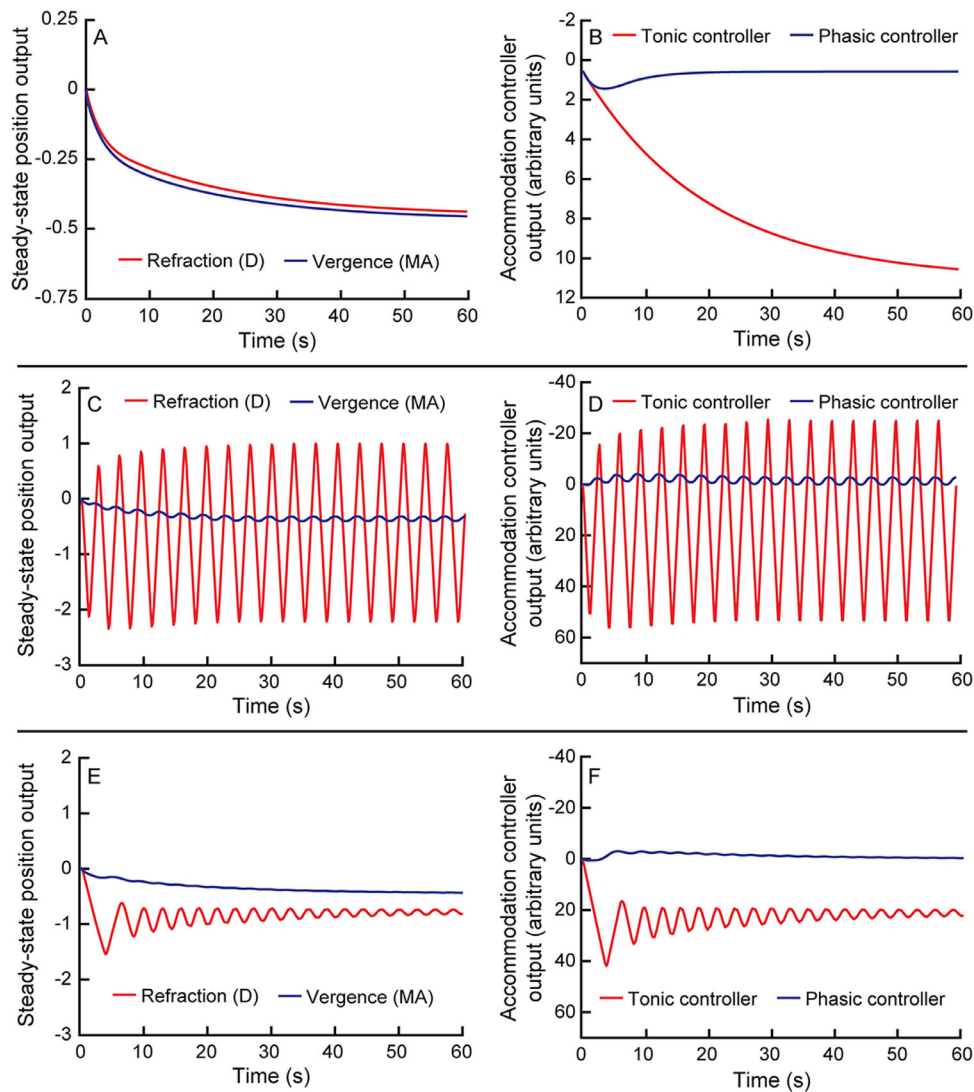


**FIGURE 8.** Control engineering model simulations of accommodation and convergence plotted as a function of time for 0.5 D (or MA) step-change in near vision demand. **A**, **C**, and **E** show the simulated model output for a control subject, a patient with manifest SNR and for the same patient with partially resolved SNR, respectively. **B**, **D**, and **F** show the model outputs of the phasic and tonic accommodation controllers for all the aforementioned conditions. The ordinate axes for the right-hand panels are in arbitrary units because they represent outputs of the accommodation neural controllers before feeding into the biomechanical plant for generating the final motor response.

tions. For instance, the low-frequency component of accommodative microfluctuations is known to vary with viewing condition (e.g., changes in viewing distance, pupil diameter, target luminance/contrast, etc.).<sup>24</sup> The refraction fluctuations in SNR should therefore also demonstrate similar patterns of variations with viewing condition. Irrespective of their source, the low-frequency microfluctuations are believed to aid accommodation maintaining an optimal refractive state by monitoring the associated changes in the retinal image quality within the eye's depth of focus.<sup>24,27</sup> It is unlikely that the refraction fluctuations in SNR perform any such role in these patients. If any, the refractive fluctuations in SNR are deleterious to the patient's retinal image quality and visual performance as their magnitude far exceeds the typical depth of focus of humans ( $\sim 0.5\text{D}$ ).<sup>28</sup>

As indicated by the model simulations, these fluctuations in refraction may largely reflect the undesired motor consequence of a maintained adaptive response of blur-

driven accommodation (Fig. 8, Table 2), quite unrelated to the physiological microfluctuations of accommodation. The inability of this controller to maintain its gain coupled with very slow decay may result in the apparent myopic refraction in patients with SNR. The tonic accommodation controller has been modeled to influence the accommodative state of the eye, without having any impact on the convergence system—the accommodative-convergence cross-coupling (or the AC/A ratio) is largely driven by the phasic accommodation controller.<sup>7</sup> This may also explain why the exaggerated fluctuations were observed only in accommodation, with little or no manifestation in the convergence system (Figs. 2–5). Intuitively, these fluctuations in refraction could also be thought to arise from abnormal gain of the negative feedback loop of accommodation that is unable to reduce the error to values smaller than the depth of focus of the eye (Fig. 1), reflecting some form of an impairment in blur processing capability in patients

with SNR. However, our model simulations did not produce such fluctuations in refraction when the gain of the negative feedback loop was increased or reduced than physiological levels (Table 2). This may be so because any fluctuations arising from negative feedback represents a mismatch between the blur processing and the neural/biomechanical properties of the plant during the time when the phasic accommodation controller is active, and this is likely to result in transient under-damped oscillations in the final response that last for a few seconds before achieving a stable steady-state.<sup>29–31</sup> The fluctuations of refraction seen in SNR were not transient but sustained with more or less same amplitude over long periods of time. It is therefore unlikely that the observed fluctuations of refraction in SNR is due to alterations in the properties of the negative feedback loop of accommodation. The model simulations in Figure 8C did exhibit small but periodic fluctuations in convergence when the tonic accommodation controller parameters were set to simulate the SNR. Such fluctuations in convergence were not observed behaviorally (Figs. 2–5), and it may reflect the limitation in the resolution of the photorefractor device used to record the convergence data in this study. The RMS deviation of convergence in the simulations was close to the resolution of the gaze tracker. It is possible that all patients in this cohort were SNR with only the accommodation component affected. If they had SNR with all three components involved, the result of the near triad would have been different.

### Impact of Modified Optical Fogging on SNR

The modified optical fogging technique intends to relieve spasm by making the patient perform a near task with their distance correction, if needed, and near-addition that is close to the expected negative relative accommodation value to maximally relax accommodation, followed by binocular defogging for distance (S. Roy et al., unpublished observations, 2019). This technique was successful in reducing the vacillating retinoscopy reflex and stabilizing the visual acuity of 20 of the 45 patients that participated in the larger cohort study (S. Roy et al., unpublished observations, 2019). Across the 15 patients tested here, the median change in manifest refraction and RMS deviation between clinical presentation and after optical fogging was 36.6% (median after therapy  $[-1.04\text{ D}]/\text{median at clinical presentation} [-1.64\text{ D}] = 36.6\%$ ) and 62.4% (median after therapy  $[0.41\text{ D}]/\text{median at clinical presentation} [1.09\text{ D}] = 62.4\%$ ), respectively (Figs. 3 and 4). The relief in SNR after the modified optical fogging technique was therefore partial, with the therapy having a larger impact in reducing the refraction fluctuations than the mean value itself. This behavior was modeled by reducing the gain and shortening the decay time constant of the tonic accommodation controller (Fig. 8, Table 2), suggesting that the optical therapy may work by facilitating the decay of the adaptive component of blur-driven accommodation that otherwise builds-up with near task in these patients. Empirical measures of tonic accommodation and its change with optical fogging needs to be undertaken in these patients to test this hypothesis.<sup>32,33</sup>

### Study Limitations

This study had four limitations. First, the visual acuity and clinical refraction data of patients with SNR were not methodically documented at all visits in the clinical records (Table 1). Thus, apart from providing general trends, we are

unable to connect these data with the corresponding objective findings of the near-triad obtained here. Further studies addressing this specific question are currently underway in the laboratory. Second, the scaling of the refraction data using the ethnicity-specific defocus calibration factor<sup>16</sup> and for the pupil diameter of the individual (especially for the pupil dilation with cycloplegia, vis-à-vis all others wherein the pupil diameter was similar [Figs. 2, 4, and 5])<sup>34</sup> did not account for the absolute values of refraction recorded by the photorefractor. We therefore cannot interpret the absolute values of manifest refraction obtained using photorefractor and rely on clinical refraction procedures for this information (Fig. 2). Similarly, the scaling of eye position using the population average Hirschberg ratio (11.8°/mm) in-built into the photorefractor does not account for individual variability in the angle kappa, and, hence, interpretation of the absolute values of vergence is also not possible. These issues of calibration could potentially also explain the relatively large inter-subject variability in the absolute values of manifest refraction and vergence shown in Fig. 4 of this study. Third, the engineering model used here did not include the pupils, and its modeling therefore remains incomplete in SNR. Previous models of synkinetic behavior of all three components of the near triad cannot be used due to lack of pertinent details in the relevant publications.<sup>35–37</sup> Given the similarity in neural architecture of the three components of near triad, the pupil simulations may also show stable responses in SNR, despite exaggerated accommodative fluctuations. Fourth, the control experiment describing the differences in the characteristics of the refraction fluctuations with different refractive error types were conducted only on ten subjects (five myopes and five hypermetropes; Fig. 7). This data therefore only provides a preliminary proof of concept on the uniqueness of the refractive fluctuations to the SNR and needs replication in a larger cohort.

### Acknowledgments

The authors thank all the participants of this study. The authors also acknowledge the support of Clifton Schor from the University of California Berkeley School of Optometry for insights into the controls engineering model of accommodation and convergence interaction and Navaneetha Ampolu from L V Prasad Eye Institute for support with data collation.

Supported by the Prof Brien Holden Eye Research Centre, Hyderabad Eye Research Foundation, L V Prasad Eye Institute, Hyderabad, India.

Disclosure: **S.R. Bharadwaj**, None; **S. Roy**, None; **P.N. Satgunam**, None

### References

- Schor CM, Ciuffreda KJ. *Vergence Eye Movements: Basic and Clinical Aspects*. Boston: Butterworth Publishers; 1983.
- Goldstein JH, Schneekloth BB. Spasm of the near reflex: a spectrum of anomalies. *Surv Ophthalmol*. 1996;40:269–278.
- Hyndman J. Spasm of the near reflex: literature review and proposed management strategy. *J Binocular Vis Ocular Motility*. 2018;68:78–86.
- Rutstein RP, Daum KM. Anomalies of Accommodation. In: Rutstein RP, Daum KM (Eds.), *Anomalies of Binocular Vision: Diagnosis and Management*. St. Louis: Mosby-Year Book, Inc.; 1998:61–94.

5. Daum KM. Accommodative dysfunction. *Doc Ophthalmol Adv Ophthalmol*. 1983;55:177–198.
6. Satgunam P. Relieving accommodative spasm: two case reports. *Optom Vis Perform*. 2018;6:207–212.
7. Schor C. The influence of interactions between accommodation and convergence on the lag of accommodation. *Ophthalm Physiol Optics*. 1999;19:134–150.
8. Eadie AS, Carlin PJ. Evolution of control system models of ocular accommodation, vergence and their interaction. *Med Biol Eng Comput*. 1995;33:517–524.
9. Schor C, Horner D. Adaptive disorders of accommodation and vergence in binocular dysfunction. *Ophthalm Physiol Optics*. 1989;9:264–268.
10. Kanda H, Kobayashi M, Mihashi T, Morimoto T, Nishida K, Fujikado T. Serial measurements of accommodation by open-field Hartmann-Shack wavefront aberrometer in eyes with accommodative spasm. *Jpn J Ophthalmol*. 2012;56:617–623.
11. Ninomiya S, Fujikado T, Kuroda T, et al. Wavefront analysis in eyes with accommodative spasm. *Am J Ophthalmol*. 2003;136:1161–1163.
12. Abrahamsson M, Ohlsson J, Bjorndahl M, Abrahamsson H. Clinical evaluation of an eccentric infrared photorefractor: the PowerRefractor. *Acta Ophthalmol Scand*. 2003;81:605–610.
13. Bharadwaj SR, Candy TR. Cues for the control of ocular accommodation and vergence during postnatal human development. *J Vis*. 2008;8:14.1–16.
14. Bharadwaj SR, Wang J, Candy TR. Pupil responses to near visual demand during human visual development. *J Vis*. 2011;11:6.
15. Bharadwaj SR, Sravani NG, Little JA, et al. Empirical variability in the calibration of slope-based eccentric photorefraction. *J Opt Soc Am A Opt Image Sci Vis*. 2013;30:923–931.
16. Blade PJ, Candy TR. Validation of the PowerRefractor for measuring human infant refraction. *Optom Vis Sci*. 2006;83:346–353.
17. Schaeffel F, Wilhelm H, Zrenner E. Inter-individual variability in the dynamics of natural accommodation in humans: relation to age and refractive errors. *J Physiol*. 1993;461:301–320.
18. Sravani NG, Nilagiri VK, Bharadwaj SR. Photorefraction estimates of refractive power varies with the ethnic origin of human eyes. *Sci Rep*. 2015;5:7976.
19. Ntodie M, Bharadwaj SR, Balaji S, Saunders KJ, Little JA. Comparison of three gaze position calibration techniques in first purkinje-image based eye trackers. *Optom Vis Sci*. 2019;96:587–598.
20. Schor CM. A dynamic model of cross-coupling between accommodation and convergence: simulations of step and frequency responses. *Optom Vis Sci*. 1992;69:258–269.
21. Hung GK. Adaptation model of accommodation and vergence. *Ophthalm Physiol Optics*. 1992;12:319–326.
22. Hung GK, Ciuffreda KJ. Sensitivity analysis of relative accommodation and vergence. *IEEE Trans Bio-Med Eng*. 1994;41:241–248.
23. Laidlaw DA, Tailor V, Shah N, Atamian S, Harcourt C. Validation of a computerised logMAR visual acuity measurement system (COMPlog): comparison with ETDRS and the electronic ETDRS testing algorithm in adults and amblyopic children. *Br J Ophthalmol*. 2008;92:241–244.
24. Charman WN, Heron G. Microfluctuations in accommodation: an update on their characteristics and possible role. *Ophthalm Physiol Optics*. 2015;35:476–499.
25. Stark L, Campbell FW, Atwood J. Pupil unrest: an example of noise in a biological servomechanism. *Nature*. 1958;182:857–858.
26. Walsh G, Charman WN. Visual sensitivity to temporal change in focus and its relevance to the accommodation response. *Vis Res*. 1988;28:1207–1221.
27. Kotulak JC, Schor CM. A computational model of the error detector of human visual accommodation. *Biol Cybernetics*. 1986;54:189–194.
28. Campbell FW. The depth of focus of the human eye. *J Physiol*. 1954;125:29–30P.
29. Bharadwaj SR, Schor CM. Dynamic control of ocular disaccommodation: first and second-order dynamics. *Vis Res*. 2006;46:1019–1037.
30. Bharadwaj SR, Schor CM. Initial destination of the disaccommodation step response. *Vis Res*. 2006;46:1959–1972.
31. Schor CM, Bharadwaj SR. Pulse-step models of control strategies for dynamic ocular accommodation and disaccommodation. *Vis Res*. 2006;46:242–258.
32. Rosenfield M, Ciuffreda KJ, Hung GK, Gilmartin B. Tonic accommodation: a review. I. Basic aspects. *Ophthalm Physiol Optics*. 1993;13:266–284.
33. Rosenfield M, Ciuffreda KJ, Hung GK, Gilmartin B. Tonic accommodation: a review. II. Accommodative adaptation and clinical aspects. *Ophthalm Physiol Optics*. 1994;14:265–277.
34. Wu Y, Thibos LN, Candy TR. Two-dimensional simulation of eccentric photorefraction images for ametropes: factors influencing the measurement. *Ophthalm Physiol Optics*. 2018;38:432–446.
35. Balaban CD, Kiderman A, Szczupak M, Ashmore RC, Hoffer ME. Patterns of pupillary activity during binocular disparity resolution. *Frontiers Neurol*. 2018;9:990.
36. McDougal DH, Gamlin PD. Autonomic control of the eye. *Compr Physiol*. 2015;5:439–473.
37. Myers GA, Stark L. Topology of the near response triad. *Ophthalm Physiol Optics*. 1990;10:175–181.